Cellular Signalling 62 (2019) 109339

Contents lists available at ScienceDirect

Cellular Signalling

journal homepage: www.elsevier.com/locate/cellsig

Effects of PP2A/Nrf2 on experimental diabetes mellitus-related cardiomyopathy by regulation of autophagy and apoptosis through ROS dependent pathway

Yanhui Guan[a], Lichun Zhou[a], Yu Zhang[a], Huiqin Tian[a,b], Anqi Li[a], Xiuzhen Han[a,c,*]

[a] Department of Pharmacology, School of Pharmaceutical Sciences, Shandong University, 44 West Wenhua Road, Jinan 250012, China
[b] Department of Pharmacology, Shandong college of Traditional Chinese Medicine, 508 East Binhai road, Yantai 264199, China
[c] Key Laboratory of Chemical Biology of Natural Products, Ministry of Education, Shandong University, Jinan, China

ARTICLE INFO

Keywords:
Diabetes mellitus-related cardiomyopathy
PP2A
ROS
Nrf2
Autophagy
Apoptosis

ABSTRACT

Diabetes mellitus-related cardiomyopathy (DMCMP) has been defined as ventricular dysfunction that occurs in diabetic patients independent of a recognized cause such as coronary artery disease or hypertension. Mechanisms underlying DMCMP have not been fully elucidated. In this study, the roles of protein phosphatase 2A/nuclear factor NF-E2-related factor 2 (PP2A/Nrf2) in experimental DMCMP induced by high glucose were studied in vitro and in vivo. The results showed that high glucose could induce experimental DMCMP and increase ROS generation, increase the expression and nuclear translocation of Nrf2, down-regulate the expression of PI3K/Akt/mTOR and up-regulate the expression of ERK, and activate the autophagy of cardiomyocytes. The activity or expression of PP2A in DMCMP increased. PP2A could up-regulate the expression of Nrf2 and promote cardiomyocytes autophagy and apoptosis. Inhibition of PP2A could reduce the expression of Nrf2 and inhibit the autophagy and apoptosis of cardiomyocytes. The results suggested that hyperglycemic-induced experimental DMCMP may be related to up-regulating the expression of Nrf2 through PP2A/Nrf2 pathway. These results will be helpful to elucidate the pathogenesis and mechanism of DMCMP and find targets for the development of new drugs to prevent or treat DMCMP.

1. Introduction

Diabetes mellitus-related cardiomyopathy (DMCMP) was originally described as a dilated phenotype with eccentric left ventricular (LV) remodeling and systolic LV dysfunction. However, recent clinical studies on DMCMP mainly describe a restrictive phenotype with concentric LV remodeling and diastolic LV dysfunction [1]. It is characterized by diastolic abnormalities in early stage and later by heart failure in the absence of dyslipidaemia, hypertension and coronary artery disease [2,3]. Multiple potential mechanisms have been implicated in the pathophysiology of DMCMP. Although depicted as separate mechanisms, these pathways interact with each other in complex ways. Examples include: (1) increased fatty acid oxidation and lipotoxicity may promote mitochondrial dysfunction; (2) mitochondrial dysfunction and endoplasmic reticulum stress may increase apoptosis; (3) oxidative stress, increased advanced glycation end products (AGE) signaling and inflammation may promote expression of pro-fibrotic genes or apoptosis [4]. DMCMP is known to relate to oxidative stress that is due to a severe imbalance between reactive oxygen species (ROS) and/or reactive nitrogen species (RNS) generation and their clearance by antioxidant defense systems [5]. Therefore, it is significant to elucidate some of the molecular and cellular mechanisms via studying the ROS and related pathways that may help struggle against DMCMP [6].

Transcription factor nuclear factor NF-E2-related factor 2 (Nrf2) is a master regulator of cellular responses against environmental stresses. Nrf2 induces the expression of detoxification and antioxidant enzymes, and Kelch-like ECH-associated protein 1 (Keap1), an adaptor subunit of Cullin 3-based E3 ubiquitin ligase, regulates Nrf2 activity [7]. As an important cellular redox sensor, Keap1 causes Nrf2 to be degraded through the ubiquitin-proteasome pathway. In the presence of oxidative or electrophilic stress, critical cysteine thiols of Keap1 are modified/oxidized and Keap1 loses its ability to ubiquitinate Nrf2 and Nrf2 degradation ceases. Nrf2 is thus stabilized and translocated to the nucleus, resulting in a coordinated activation of gene expression [8,9]. In addition, new sets of Nrf2 target genes whose products are involved in cell

* Corresponding author at: Department of Pharmacology, School of Pharmaceutical Sciences, Shandong University, 44 West Wenhua Road, Jinan 250012, China.
E-mail address: xzyhan@sdu.edu.cn (X. Han).

https://doi.org/10.1016/j.cellsig.2019.06.004
Received 20 January 2019; Received in revised form 2 June 2019; Accepted 4 June 2019
Available online 05 June 2019

proliferation and differentiation but not necessarily in the regulation of oxidative stress have been identified by analyses of the genome-wide distribution of Nrf2 [10]. Study has indicated Nrf2 may have an important protective effect on DMCMP. Genetic activation of Nrf2 signaling by Keap1 gene hypomorphic knockdown (Keap1flox/−) markedly suppresses the onset of diabetes [8]. By using Nrf2-KO mouse model, the important role of Nrf2 in protecting various organs including the heart from diabetes has been extensively approved [5]. Enhanced Nrf2 activation worsens insulin resistance, impairs lipid accumulation in adipose tissue, and increases hepatic steatosis in leptin-deficient mice [11]. In addition, Nrf2 deficiency prevents from reductive stress-induced hypertrophic cardiomyopathy. Sustained activation of Nrf2 may cause a significant decrease of protein oxidation in association with the induction of chronic reducing stress, which in turn causes deubiquitination and downstream protein degradation pathways, resulting in the development of cardiac hypertrophy and remodeling [12]. Meanwhile, there is a close relationship between Nrf2, autophagy, and apoptosis through the relationship with ROS. The tight interactions between ROS and autophagy reflects in two aspects: the induction of autophagy by oxidative stress and the reduction of ROS by autophagy [13]. It has been found that oxidative stress induces apoptosis of diabetic cardiomyocytes through multiple pathways, such as direct activation of mitochondrial apoptosis pathway, tumor necrosis factor α (TNF-α) and death receptor pathway, p53 apoptosis pathway and p38 mitogen activated protein kinases (MAPK) pathway [14].

Protein phosphatase 2A (PP2A) is a central cardiac phosphatase that regulates diverse myocyte functions through a host of target molecules. It is composed of a catalytic subunit (C), a structural subunit (A), and a regulatory/variable B-type subunit [15]. Study showed that, in high glucose (HG)-cultured cardiomyocytes, phosphorylation of GSK-3β was decreased, while that of the PP2A catalytic subunit C (PP2Ac) and IKK/IκBα was increased, followed by NF-κB nuclear translocation and apoptosis. These findings demonstrated that Atorvastatin protected cardiomyocytes from HG-induced apoptosis and alleviated experimental DMCMP by regulating the GSK-3β-PP2A-NF-κB signaling pathway [16]. Recent study has reported that the relationship between ROS and promotion of chemoresistance via nitration of PP2A and excess ROS can promote oxidative inactivation of PP2A [17–19]. PP2A can participate in insulin activation and improve insulin resistance in metabolism [20]. However, whether PP2A/Nrf2 can protect cardiomyocytes in the hyperglycemia environment is not clear. Thus, the roles and mechanisms of PP2A/Nrf2 in experimental DMCMP were studied in vitro and in vivo for the first time in order to lay the foundation for the development of the drugs for the prevention and treatment of DMCMP.

2. Materials and methods

2.1. Materials

Dulbecco's modified Eagle's medium (DMEM) was purchased from Gibco BRL (Grand Island, NY, USA). Fetal bovine serum (FBS) was from Tianjin Kangyuan Biotech Co., Ltd. (Tianjin, China) ; LysoTracker Green fluorescent dye (LTG) was purchased from Invitrogen (California, USA); Acridine orange (AO) and Hoechst 33342 solution were from Beyotime Biotechnology (Shanghai, China); Annexin V-FITC/propidium iodide (PI) cell apoptosis detection kit was from Beijing 4A Biotech Co., Ltd. (Beijing, China); Malondialdehyde (MDA), Glutathione peroxidase (GSH-Px), Superoxide dismutase (SOD), Catalase (CAT), and Total nitric oxide synthase (NOS) detection kits were from Nanjing Jiancheng Bioengineering Institute (Nanjing, China); Sodium citrate buffer (0.1 M, pH 4.5) was from Solarbio Biotech Co., Ltd. (Beijing, China); Streptozocin (STZ) was from Sigma; p-Akt and Akt were from Santa Cruz Biotechnolog (Santa Cruz, USA); Bcl-2, Bax, PARP, caspase-3, PI3K, ERK, p-ERK, p-mTOR, mTOR, p62, and β-actin were from Cell Signaling Technology (Cell Signaling, USA); LC3B, Nrf2, and HIF-1α were from Sigma. Okadaic acid (OA , 98%) was from J&K Scientific LTD (Beijing, China) ; Fingolimod hydrochloride (FTY720) was from Shanghai Sixin Biotechnology Co., Ltd. ; Ad-PP2A/Ad-dn-PP2A were presented by Professor Shile Huang, Health Sciences Center, Louisiana State University.

2.2. Cell culture

Rat cardiac H9c2 cells (ATCC, Rockville, MD, USA) were cultured in DMEM supplemented with 10% heat-inactivated FBS, 100 μg/ml streptomycin, and 100 unit/ml penicillin at 37 °C in a humidified atmosphere (5% CO_2). The cells were fed every 1–2 days and subcultured once they reached about 80–90% confluence. Cells were plated at an appropriate density according to each experimental design, and the cells were in the exponential phase of growth before exposure to drugs in all experiments.

2.3. Cell viability in vitro

H9c2 cells were seeded in 96-well plates at a density of 3000 cells/well. Following overnight adherence, cells were incubated with glucose (5, 10, 25, and 50 mmol/L) in DMEM supplemented with 10% fetal bovine serum at 37 °C for 24, 48, and 72 h. Then cell proliferation was determined by MTT assay. Cells were treated with MTT solution (final concentration, 0.5 mg/ml) for 4 h. The supernatants were removed carefully, followed by the addition of 150 μl DMSO to each well to dissolve the precipitate. Then, the absorbance was measured at 570 nm in a microplate reader (Synergy HT).

2.4. Cell morphological analysis

H9c2 cells were seeded at a density of 2.5×10^4 cells/well in a 24-well plate and grew overnight at 37 °C in a humidified incubator with 5% CO_2. The next day, cells were pretreated with/without glucose (50 mmol/L) for 72 h. After indicated incubation, Giemsa staining [21] and cell morphology was examined under an inversion microscope. The cell area of each group was measured by the software of image Pro Plus, each group randomly selected 50 cells and calculated the average value (×200).

2.5. Analysis for generation of ROS

The production of ROS was measured by detecting the fluorescent intensity of oxidant-sensitive probe DCFH-DA, which was a stable nonfluorescent molecule that passively diffuses into cells, where the acetate could be cleaved by intracellular esterase to produce a polar diol that was well retained within the cells. H9c2 cells were seeded at a density of 2.5×10^4 cells/well in 24-well plate. The next day, cells were pretreated with/without NAC (5 mmol/L) for 2 h followed by incubation with glucose (50 mmol/L) for another 72 h. Then cells were loaded with DCFH-DA (10 μmmol/L) as per the manufacturer's protocol for 0.5 h. Fluorescent intensity was recorded by excitation at 485 nm and emission at 535 nm using a Wallac 1420 Multilabel Counter (Wallac, Turku, Finland). Cells in the 24-well plate were observed under a fluorescence microscope.

2.6. AO and LTG staining

AO and LTG staining were applied to observe the autophagy in cells pretreated with glucose. H9c2 cells were seeded in 24-well plates at density of 2.5×10^4 cells/well. After the corresponding treatment, the cells were stained with AO or LTG. Morphologic changes were observed and photographed under the fluorescence microscope (Olympus, Japan). AO was used to evaluate the abundance of autophagic vacuoles in the cells [22]. LTG is a green fluorescent dye used to dye acidic chambers in living cells.

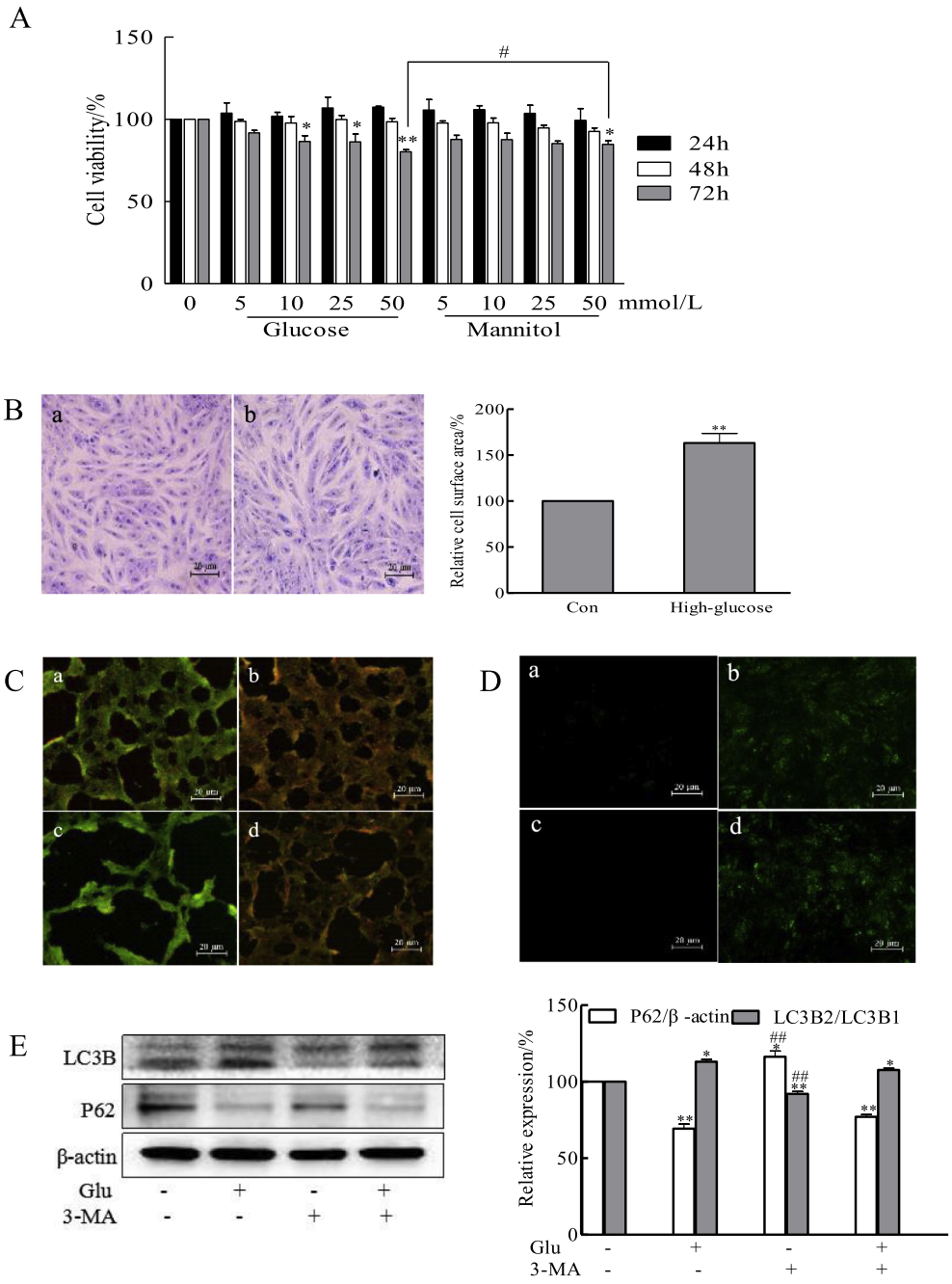

Fig. 1. Effects of high glucose on H9c2s cells. (A) Cell viability. H9c2 cells were treated with different concentrations (0, 5, 10, 25, and 50 mmol/L) glucose in different times(24, 48, and 72 h) before cell viability was measured by MTT assay. $^{*}P < .05$, $^{**}P < .01$, vs. control cells. $^{\#}P < .05$, vs. mannitol cells. Results are presented as means ± SEM ($n = 6$). (B) Cell morphology. H9c2 cells were treated without (a) or with (b) high glucose (50 mmol/L) for 72 h. Cells were stained with Giemsa staining and counted cell surface area. $^{**}P < .01$, vs. control cells. Results are presented one of three independent experiments. (C) AO staining. H9c2 cells were incubated with 3-MA (5 mmol/L) for 2 h, then treated with glucose (50 mmol/L) for 72 h. Cell pictures were taken under a fluorescent microscope (×200). (a) Control; (b) High glucose; (c) 3-MA; (d) 3-MA + High glucose. Results are presented one of three independent experiments. (D) LTG staining. H9c2 cells were pretreated with 3-MA or glucose as above. Cell pictures were taken under a fluorescent microscope (×200). (a) Control; (b) High glucose; (c) 3-MA; (d) 3-MA + High glucose. Results are presented one of three independent experiments. (E) Western blotting was used to detect the expression of LC3B and P62. Results are presented as means ± SEM of three independent experiments. $^{*}P < .05$, $^{**}P < .01$, vs. control cells. $^{\#}P < .05$, $^{\#\#}P < .01$, vs. High-glucose.

2.7. Western blotting

A total of 30 μg of myocyte proteins were separated by 10% SDS-PAGE, and then transferred to polyvinylidene difluoride membranes (PVDF) (Millipore Corporation, USA) in Tris-glycine buffer. After blocking with 5% (*w/v*) non-fat dry milk in 20 mmol/L Tris-buffered saline containing 0.1% (*v*/v) Tween-20 (TBST) for 4 h, the membrane was incubated with the appropriate primary antibodies at 4 °C overnight and then washed three times. After incubation with secondary antibodies (ZSGB-BIO, China) at room temperature for 1 h, the proteins were detected with enhanced chemiluminescence and quantified using a Gel Doc 2000 Imager (Bio-Rad, USA). Protein expression was normalized to β-actin.

2.8. Adenovirus transfection of PP2A

H9c2 cells were seeded at a density of 10×10^4 cells/well in 6-well plate. The next day, cells were pretreated with/without NAC (5 mmol/L) for 2 h followed by incubation with OA/FTY720 or Ad-PP2A/Ad-dn-PP2A for another 24 h (control cell was treated with LacZ), then cells were pretreated with/without glucose (50 mmol/L) for 72 h.

2.9. Hoechst 33342 staining

H9c2 cells were seeded at a density of 2.5×10^4 cells/well in 24-well plate. Then pretreated with/without NAC (5 mmol/L) for 2 h followed by incubation with OA/FTY720 or Ad-PP2A/Ad-dn-PP2A for another 24 h, followed by glucose (50 mmol/L) for another 72 h. Cells were fixed with 4% paraformaldehyde for 10 min, followed with 1% Triton-X-100 for 10 min. Hoechst 33342 stain at concentration of

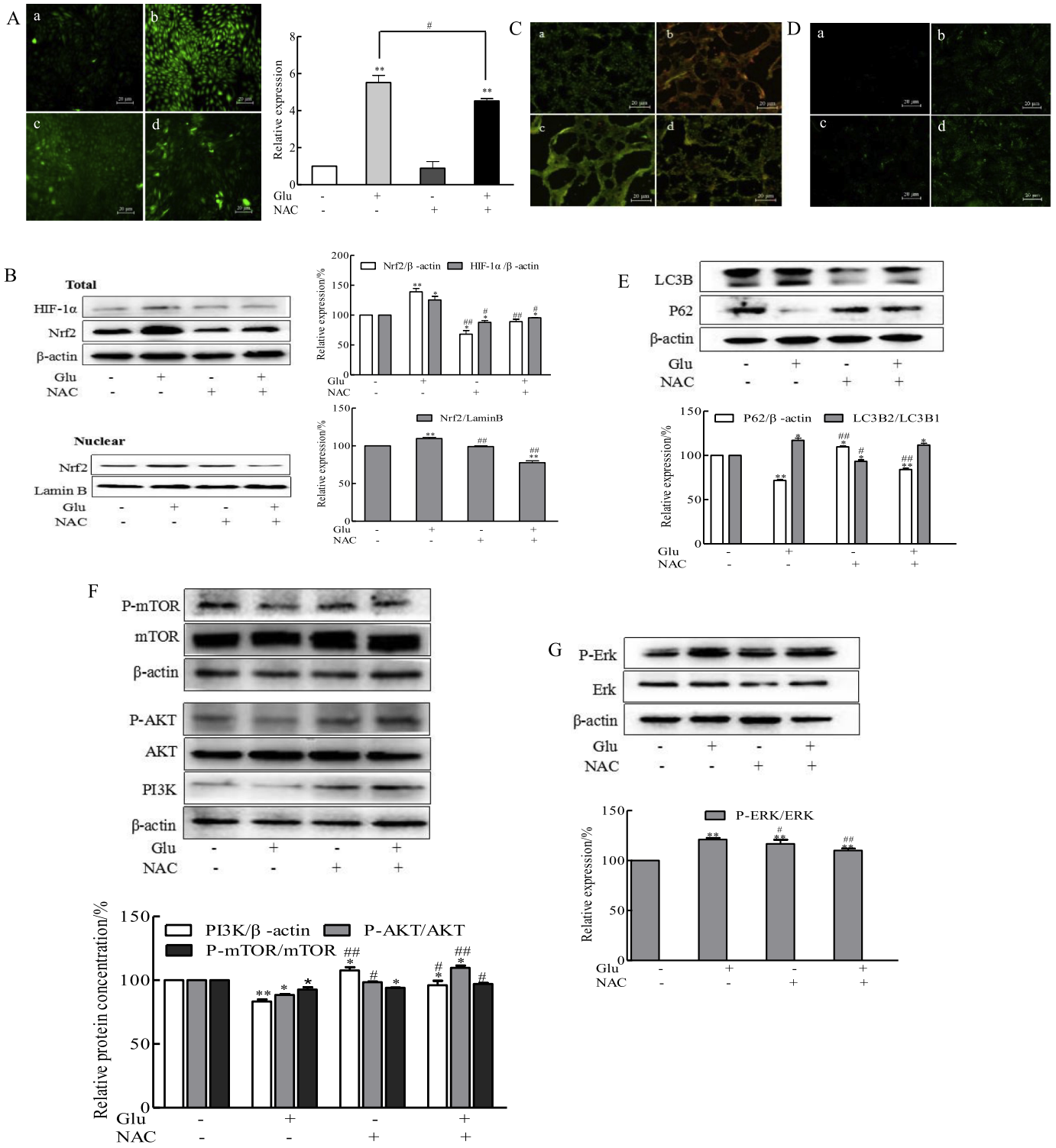

Fig. 2. ROS generation and autophagy in high-glucose induced H9c2 cells. H9c2 cells were pretreated with NAC (5 mmol/L) for 2 h, then treated with glucose (50 mmol/L) for 72 h. (A) The ROS level was determined by assaying the fluorescent product 2′, 7′-dichlorofluorescein (DCF) from 2′, 7′-dichlorofluorescin diacetates (DCFH-DA). The images were captured by fluorescence microscopy using identical exposure settings (×200). Results are presented one of three independent experiments. (B) Western blotting was used to detect the expression of Nrf2 and HIF-1α. Results are presented as means ± SEM of three independent experiments. $^{*}P < .05$, $^{**}P < .01$, vs. control cells. $^{\#}P < .05$, $^{\#\#}P < .01$, vs. High-glucose. (C) Cells were stained with AO. (a) Control, (b) High glucose, (c) NAC, (d) NAC + High glucose. Results are presented one of three independent experiments. (D) Cells were stained with LTG. (a) Control, (b) High glucose, (c) NAC, (d) NAC + High glucose. Results are presented one of three independent experiments. (E, F, G) Western blotting was used to detect the expression of LC3B, P62, PI3K, p-Akt, p-mTOR, and P-ERK. Results are presented as means ± SEM of three independent experiments. $^{*}P < .05$, $^{**}P < .01$, vs. Control; $^{\#}P < .05$, $^{\#\#}P < .01$, vs. High-glucose.

10 mg/mL was used to dye the nucleus of H9c2 cells.

2.10. Flow cytometric detection of apoptosis

H9c2 cells were seeded at a density of 10×10^4 cells/well in 6-well plate, treated with OA/FTY720 or Ad-PP2A/Ad-dn-PP2A and harvested as described above. Cells were washed twice with DPBS and stained with Annexin-V/PI staining kit following the manufacturer's instructions. Cells were analyzed using a FACSCanto II (BD Biosciences). Quantification of viable (double-negative), early apoptotic (annexin V-positive), late apoptotic (annexin V and PI double-positive) and necrotic cells (PI-positive) was performed using FlowJo v10.4.1 (FlowJo, LLC).

2.11. In vivo animal model

Male Kunming mice, 6–8 weeks, weighed 18-22 g were purchased from the Experimental Animal Center, Shandong University. The research protocol was in accordance with the institutional guidelines of the Animal Care and Use Committee at Shandong University. Thirty-six mice were fed with high sugar and high fat diet for 4 weeks. Then the mice fasted overnight, each mouse was injected with STZ at a concentration of 30 mg/kg for 3 days. There were 32 mice whose blood glucose was stable at 10.9 mmol/L, then randomly divided into 3 groups for follow-up experiment. Normal diet was used in the blank group, and OA group received intraperitoneal injection of 2 μg/kg/d, FTY720 group was intraperitoneally injected with 1 mg/kg/d. Fasting body weight and blood glucose were measured every 7 days until the end of the experiment.

2.12. Tissue collection and serum analysis

At the end of the experiment, all mice were sacrificed, and each mouse's blood was taken in the 1.5 ml EP tube. After resting 2 h at room temperature, blood was centrifuged at low temperature (13,000 r/min) for 15 min, and the upper serum was taken in the new EP tube and used for enzyme activity assays. The heart tissue of each mouse was collected and used for Western blotting.

2.13. Statistical analyses

Data were described as the mean ± SEM and analyzed by one-way ANOVA. A P value $< .05$ was considered statistically significant. Statistical analysis was performed using the SPSS/Win13.0 software (SPSS, Inc., Chicago, IL).

3. Results

3.1. Effects of high glucose on H9c2 cells

To analyze effects of high glucose on the proliferation of H9c2 cells, cell viabilities were evaluated with MTT assay. As shown in Fig. 1A, H9c2 cells were incubated with glucose at different concentrations and mannitol was used as osmotic pressure control. When incubation for 24 and 48 h, glucose had little effect on the viability of H9c2 cells ($P > .05$). But incubation for 72 h, the proliferation of H9c2 cells was significantly inhibited with the increase of glucose concentration (10, 25, 50 mmol/L), and at concentration of 50 mmol/L, there was a significant difference between glucose group and mannitol group ($P < .05$). So, the subsequent experiments were carried out under the conditions of high glucose 50 mmol/L for 72 h. To further confirm whether high glucose caused cardiomyocyte damage, cells were stained with Giemsa staining solution and photographed, and cell area of each group was counted by Image Pro Plus. As shown in Fig. 1B, the surface area of H9c2 cells in high-glucose group was significantly higher than that in control group ($P < .01$).

Autophagy plays an important role in normal cardiomyocyte morphology and function. To analyze the effects of high glucose on autophagy in H9c2 cells, autophagy inhibitor 3-MA was added. As shown in Fig. 1C, the red fluorescence of H9c2 cells stained by AO in high glucose group was significantly increased, and the autophagy level increased. Incubation with 3-MA (5 mmol/L) could reduce the increase of autophagy induced by high glucose. As shown in Fig. 1D, LTG was used to further determine the effect of high glucose on autophagy, the green fluorescence intensity of lysosome in H9c2 cells was significantly increased after treated with high glucose. In addition, the expression of autophagy associated protein LC3B and P62 were detected by Western blotting. As shown in Fig. 1E, high glucose group could increase autophagy level by increasing the ratio of LC3B2/LC3B1 and decreasing the expression of P62 protein. 3-MA incubation could attenuate the upregulation of autophagy induced by high glucose.

3.2. Effects of ROS on high-glucose accumulated H9c2 cells

ROS are the main facilitators of cardiovascular complications in diabetes mellitus, and the ROS level is increased in cultured cells exposed to high glucose or in diabetic animal models [23]. As shown in Fig. 2A, the results also confirmed this point. High glucose could increase ROS generation in H9c2 cells. In order to further explore the mechanism of ROS in hyperglycemic cardiomyopathy, NAC was added as an inhibitor of ROS. As shown in Fig. 2B, compared with the control group, the expression of Nrf2 and HIF-1α increased in high glucose group. Pretreatment with NAC (5 mmol/L) could decrease the expression of Nrf2 and HIF-1α. Furthermore, the nuclear translocation of Nrf2 reduced. On this basis, we further detected the changes of autophagy and related pathways when the content of ROS changed. As shown in Fig. 2C, the red fluorescence of H9c2 cells in NAC + high glucose group was significantly decreased; indicating pretreatment with NAC could reduce the increase of autophagy induced by high glucose. Meanwhile, as LTG staining shown, when ROS generation was inhibited, the green fluorescence was obviously weakened (Fig. 2D). In addition, as shown in Fig. 2E, NAC + high glucose group could decrease autophagy level by decreasing the ratio of LC3B2/LC3B1 and increasing the expression of p62 protein.

We further detected expression of related proteins by Western blotting. As shown in Fig. 2F and G, compared with the control group, the high glucose group could inhibit the expression of PI3K, P-Akt, and P-mTOR and increase the expression of p-ERK. Compared with the high glucose group, NAC group could reverse the results.

3.3. Effects of PP2A on Nrf2 in H9c2 cells

In order to study the relationship between PP2A and Nrf2 in cardiomyocytes cultured with high glucose, and whether this is related to the change of ROS. OA, an inhibitor of PP2A, FTY720, an inducer, and Ad-PP2A/Ad-dn-PP2A were added in the experiment. As shown in Fig. 3A and B, compared with the high glucose group, the expression of Nrf2 and nuclear translocation decreased when pretreatment with NAC and/or OA was inhibited. While FTY720 could increase the expression of Nrf2 and nuclear translocation. When the expression of PP2A was inhibited and NAC was added, it was found that the expression of Nrf2 and nuclear translocation was reduced. Upregulation the expression of PP2A could increase the expression of Nrf2 and nuclear translocation. Furthermore, compared with the control group, high glucose could increase the expression of HIF-1α. Ad-dn-PP2A and NAC could significantly reduce the expression of HIF-1α compared with the high glucose group (Fig. 3C). These results suggest that there is a close relationship between PP2A, Nrf2 and ROS level in high-glucose cultured cardiomyocytes.

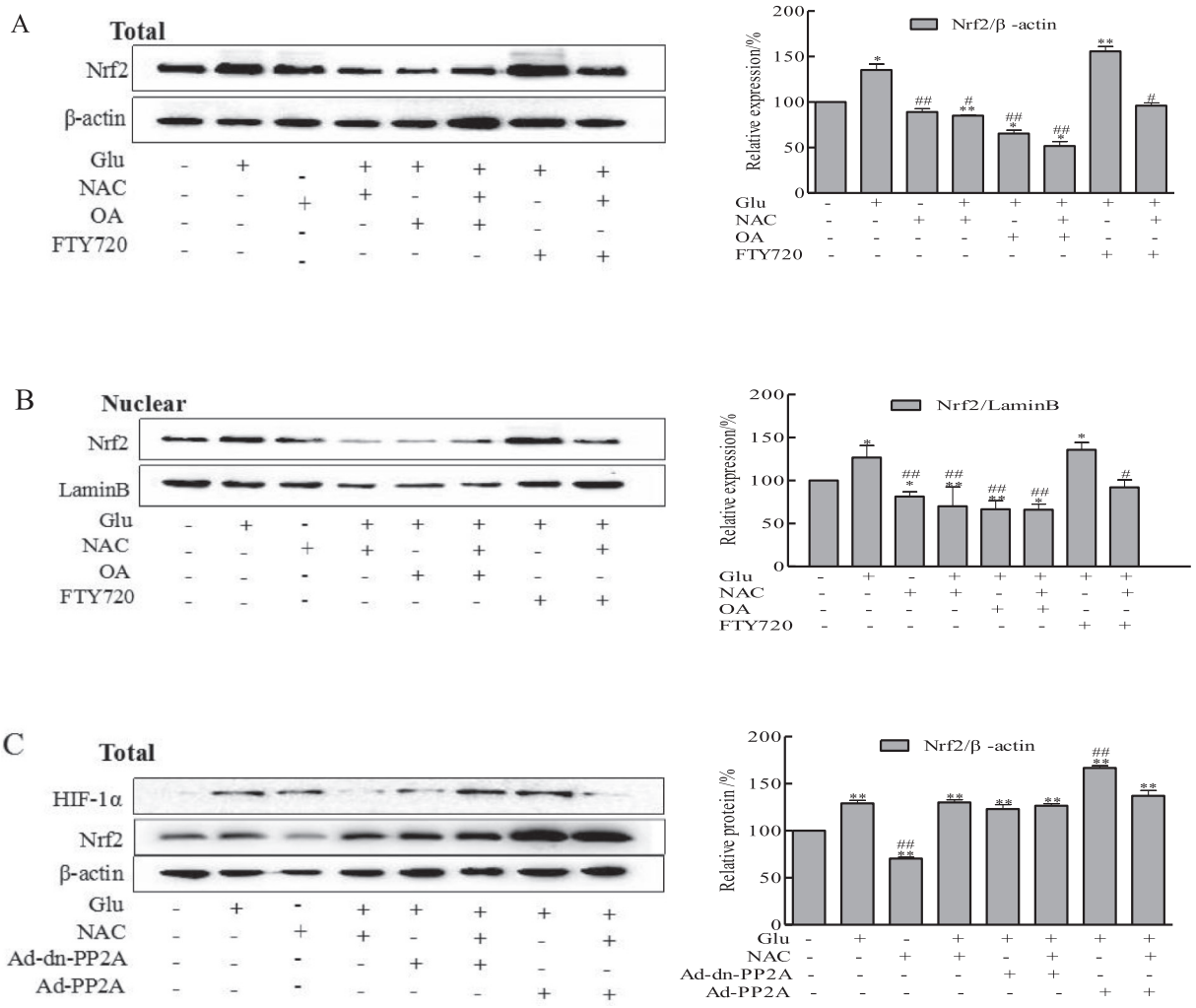

Fig. 3. Effects of PP2A on the expression of Nrf2 in H9c2 cells. H9c2 cells were pretreated without or with NAC (5 mmol/L) for 2 h, then treated with OA (20 nmol/L), FTY720 (5 mmol/L) or Ad-PP2A/Ad-dn-PP2A for 24 h, followed by treatment with glucose (50 mmol/L) for another 72 h. Western blotting was used to detect the expression of Nrf2 and HIF-1α. Results are presented as means ± SEM of three independent experiments. $^{*}P < .05$, $^{**}P < .01$, vs. Control; $^{\#}P < .05$, $^{\#\#}P < .01$, vs. High-glucose.

3.4. Effect of PP2A/Nrf2 on autophagy of H9c2 cells induced by high glucose

The above experiments confirmed that PP2A and Nrf2 were closely related to high glucose in H9c2 cells. In order to further study the relationship between PP2A/Nrf2 and autophagy, AO and LTG staining and Western blotting were used. As Fig. 4A shown, compared with the high glucose group, the red fluorescence level of OA or FTY720 group was lower. As LTG staining shown in Fig. 4B, consistent with AO staining, the green fluorescence level of OA or FTY720 group was lower than that of the high glucose group. In addition, as shown in Fig. 4C, compared with high glucose group, the ratio of LC3B2/LC3B1 decreased and p62 protein increased in OA group, the ratio of LC3B2/LC3B1 and p62 protein in FTY720 group was similar to that in high glucose group. The level of autophagy in FTY720 group decreased significantly after NAC incubation while the autophagy level in OA group was not changed. After adding Ad-PP2A/Ad-dn-PP2A in H9c2 cells induced by high glucose, as Fig. 4D and E shown, the effects were consistent with that of PP2A inhibitor and inducer. These results suggested that PP2A is closely related to ROS in regulating the level of autophagy induced by high glucose.

3.5. Effect of PP2A/Nrf2 on apoptosis of H9c2 cells induced by high glucose

In order to further study the effect of PP2A/Nrf2 on apoptosis of H9c2 cells under high glucose condition, the apoptosis in each group was detected by Hoechst 33342 staining. As shown in Fig. 5A, compared with the control group, the changes of nuclear staining in high glucose group and NAC group were not obvious. It was possible that this concentration of glucose had a weak effect on cardiomyocyte apoptosis. However, the changes of nuclear staining in OA group and FTY720 group were obvious. Compared with high glucose group, most nuclei in OA + NAC group and FTY720 group showed dense staining. Some of them showed fragmented dense staining and semilunar condensation, and apoptosis was promoted. In FTY720 + NAC group, the apoptotic bodies were significantly less, the morphology of the cells was normal, and the apoptosis was inhibited.

The expression of Bcl-2, Bax, PARP and other proteins was detected by Western blotting. As shown in Fig. 5B, compared with the control group, the expression of Bcl-2 in high glucose group was not significantly changed. The ratio of Bcl-2/Bax decreased, the expression of caspase-3 increased. The expression of cleaved-PARP was also slightly increased, but the change of cleaved-PARP/PARP was not obvious. These results suggested that glucose in this concentration can promote cardiomyocyte apoptosis. Compared with high glucose group, the ratio

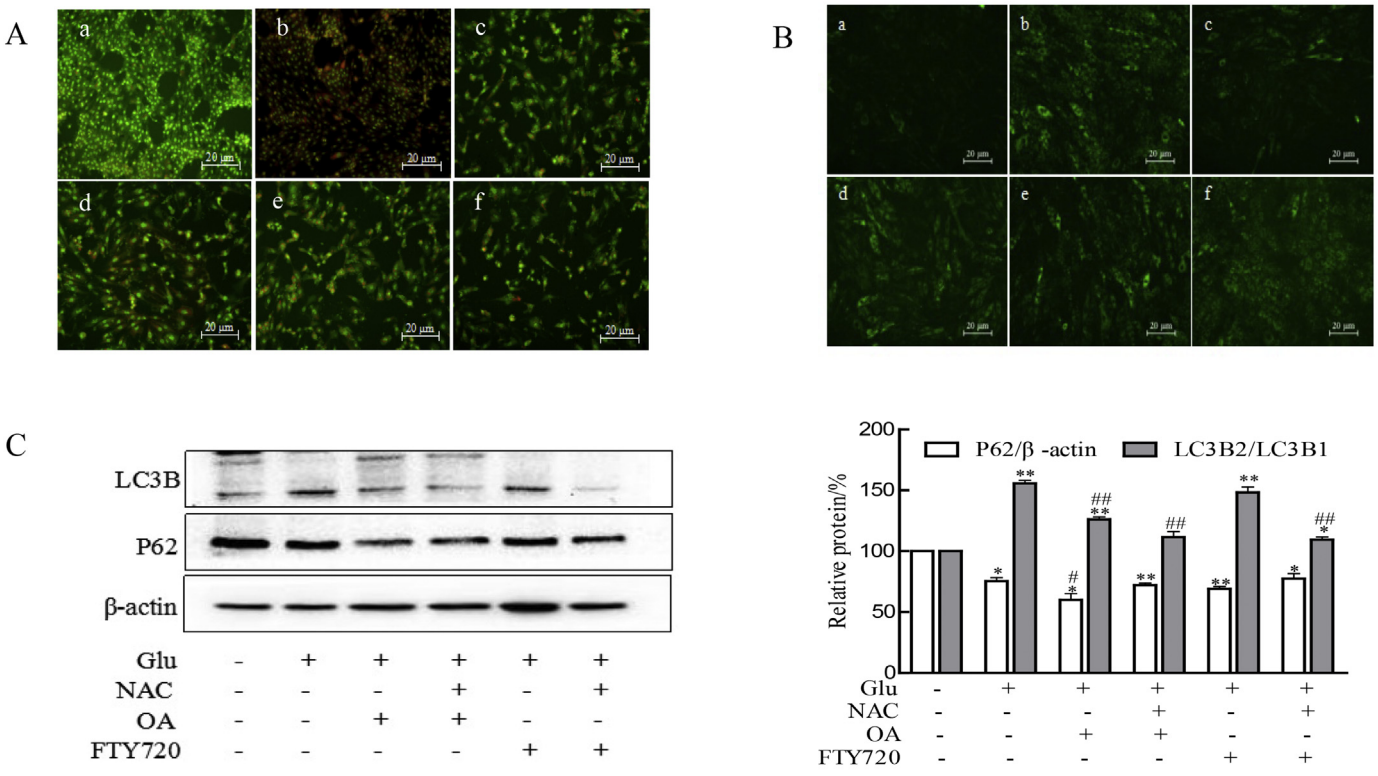

(caption on next page)

of Bcl-2/Bax in NAC and NAC + high glucose group significantly decreased, the cleaved-PARP/PARP and caspase-3 increased, which indicated that NAC promoted apoptosis. The ratio of Bcl-2/Bax significantly increased in OA group. The changes of caspase-3 were not significantly decreased in OA group, indicating that OA inhibited cardiomyocytes apoptosis induced by high glucose, while Bcl-2 was completely inhibited in OA + NAC group. Apoptosis was significantly increased, indicating that inhibition of ROS at the same time by adding NAC could enhance the decrease of Bcl-2 expression in cardiomyocytes. However, the ratio of Bcl-2/Bax in FTY720 + NAC group increased

Fig. 4. Effects of PP2A and NAC on high glucose induced autophagy in H9c2 cells. (A) AO staining. H9c2 cells were pretreated without or with NAC (5 mmol/L) for 2 h, then treated with OA (20 nmol/L) or FTY720 (5 mmol/L) for 24 h, followed by treatment with glucose (50 mmol/L) for another 72 h. Cell pictures were taken under a fluorescent microscope (×200). (a) Control; (b) High glucose; (c) OA + High glucose; (d) OA + NAC + High glucose; (e) FTY720 + High glucose; (f) FTY720 + NAC + High glucose. Results are presented one of three independent experiments. (B) LTG staining. H9c2 cells were pretreated as above. Cell pictures were taken under a fluorescent microscope (×200). (a) Control; (b) High glucose; (c) OA + High glucose; (d) OA + NAC + High glucose; (e) FTY720 + High glucose; (f) FTY720 + NAC + High glucose. Results are presented one of three independent experiments. (C) Western blotting was used to detect the expression of LC3B and P62. Results are presented as means ± SEM of three independent experiments. $^{*}P < .05$, $^{**}P < .01$, vs. Control; $^{\#}P < .05$, $^{\#\#}P < .01$, vs. high-glucose. (D) Effects of Ad-PP2A on high glucose induced autophagy in H9c2 cells. H9c2 cells were pretreated without or with NAC (5 mmol/L) for 2 h, then treated with Ad-PP2A or Ad-dn-PP2A for 24 h, followed by treatment with glucose (50 mmol/L) for another 72 h. Cell pictures stained by LTG were taken under a fluorescent microscope (×200). (a) Control; (b) High glucose; (c) Ad-dn-PP2A + High glucose, (d) Ad-dn-PP2A + NAC + High glucose, (e) Ad-PP2A + High glucose, (f) Ad-PP2A + NAC + High glucose. Results are presented one of three independent experiments. (E) Effects of PP2A and NAC on the expression of autophagy related proteins in H9c2 cells. Western blotting was used to detect the expression of LC3B and P62. Results are presented as means ± SEM of three independent experiments. $^{*}P < .05$, $^{**}P < .01$, vs. Control; $^{\#}P < .05$, $^{\#\#}P < .01$, vs. high-glucose.

significantly and the expression of caspase-3 decreased, which indicated apoptosis was inhibited compared with FTY720 group.

Apoptosis rate was detected by flow cytometry. As shown in Fig. 5C, compared with the high glucose group, the apoptosis rate of OA group decreased, while the apoptosis increased significantly after the addition of NAC. The apoptosis of FTY720 group increased, and the apoptosis of the group decreased significantly after the addition of NAC. After adding Ad-PP2A/Ad-dn-PP2A in H9c2 cells induced by high glucose, as Fig. 5D and E shown, these results were consistent with that of PP2A inhibitor and inducer. However, the effect of Ad-PP2A on the expression of capase-3 was more obvious. After adding Ad-dn-PP2A, the expression of caspase-3 was almost completely suppressed.

3.6. The changes of body weight and blood sugar levels in mice

Changes of body weight and blood sugar in mice were shown in Table 1. After STZ injection, blood glucose increased in a time-dependent manner. Compared with the control group, the body weight and blood sugar in the model group were significantly increased, indicating that the model was successful. Compared with the model group, the body weight and blood sugar in OA group were significantly increased after 6 weeks. On the contrary, blood sugar in the FTY720 group were significantly decreased.

3.7. Detection of peroxidase in serum in mice

As shown in Table 2, compared with the control group, the content of SOD and CAT in serum of the model group decreased and the ratio of MDA, MDA/SOD and NOS increased obviously, which indicated the activation of antioxidant reduction pathway. The increase of CAT content and the decrease of MDA/SOD ratio were in the OA group compared with the model group. The levels of NOS in serum of mice treated with FTY720 were significantly higher than those of model group.

3.8. Expression of Nrf2, autophagic and apoptotic protein in myocardium of mice

The results were consistent with cell experiments in vitro. As Fig. 6A shown, compared with the control group, the expression of Nrf2 and the ratio of LC3B2/LC3B1 increased and the expression of p62 decreased in model group. Compared with model group, after administration of OA, the expression of Nrf2 decreased significantly, the ratio of LC3B2/LC3B1 decreased and the expression of p62 increased. The expression of Nrf2 significantly increased after FTY720 administration while the ratio of LC3B2/LC3B1 decreased and p62 increased slightly. As Fig. 6B shown, compared with the control group, the ratio of Bcl-2/Bax increased, the expression of caspase-3 and PARP increased in model group. Compared with model group, after administration of OA, the ratio of Bcl-2/Bax decreased a little, the expression of caspase-3 and PARP decreased significantly. After FTY720 administration, the expression of Bcl-2 were almost entirely suppressed, the expression of caspase-3 and PARP decreased. The results indicated that compared with the model group, the autophagy was decreased after administration of OA and FTY720. The apoptosis of OA group was inhibited and the apoptosis of FTY720 group was increased, which may be related to the change of Nrf2 protein.

4. Discussion

Diabetes mellitus is a vastly prevalent metabolic disorder with escalating global health concerns [24]. Cardiovascular complications are the major cause of mortality and morbidity in diabetic patients [25]. Despite a growing interest in the pathophysiology of DMCMP, there are no specific guidelines for diagnosing patients or structuring a treatment strategy in clinical practice [26]. Thus, an urgent need exists to clarify the mechanism of pathogenesis. Studies have demonstrated that hyperglycemia can result in oxidative stress and is generally considered to be a key factor in the initiation of diabetic myocardial damage. Furthermore, the interplay between the autophagic and apoptotic pathways is important in the pathogenesis of DMCMP [27,28].

As redox-sensing transcription factor, Nrf2 regulates the expression of a large battery of cytoprotective genes. Study has revealed that Nrf2 and its target genes are critical regulators of cardiovascular homeostasis via the suppression of oxidative stress [29]. In our experiment, we found that the level of ROS increased under high glucose condition, the expression and nucleus translocation of Nrf2 increased, thus regulating the downstream redox pathway to protect cardiomyocytes. At the same time, it was found that the level of autophagy increased. When the production of ROS was inhibited, the expression of Nrf2 decreased and the level of autophagy decreased, suggesting that Nrf2 can also protect cardiomyocytes by regulating autophagy.

The process of autophagy is regulated by a series of complex signaling molecules. mTOR is the key protein controlling autophagy in mammals and responds to different environmental changes by changing the autophagy of cells. PI3K/Akt is the upstream signaling pathway of mTORC1 which can regulate cardiac injury during diabetes [30]. Akt phosphorylation can activate mTOR and inhibit autophagy [31]. It has been shown that Ras/Raf/MEK/ERK signaling pathway can not only induce autophagy directly by up-regulating the expression of autophagy related proteins, but also inhibit autophagy by indirectly activating the PI3K/Akt/mTOR signaling pathway [32]. On the one hand, Ras/Raf/MEK/ERK signaling pathway activates ERK under stress and directly promotes the expression of LC3II and p62, then starting autophagy in the insulin resistant diabetic heart [33]. On the other hand, it can decrease the expression of lysosomal associated membrane protein 1 (LAMP1) and LAMP2, and prevent binding with lysosome, thus inhibiting the degradation of autophagy [34]. In our experiment, high glucose might regulate the increase of Nrf2 by increasing ROS generation, and further regulate PI3K/AKT/mTOR and ERK signaling pathway to enhance autophagy. Pretreatment with NAC reversed these effects (Fig. 7A).

In addition, the results showed that whether the expression of PP2A was inhibited or increased, the cardiac myocytes remained higher

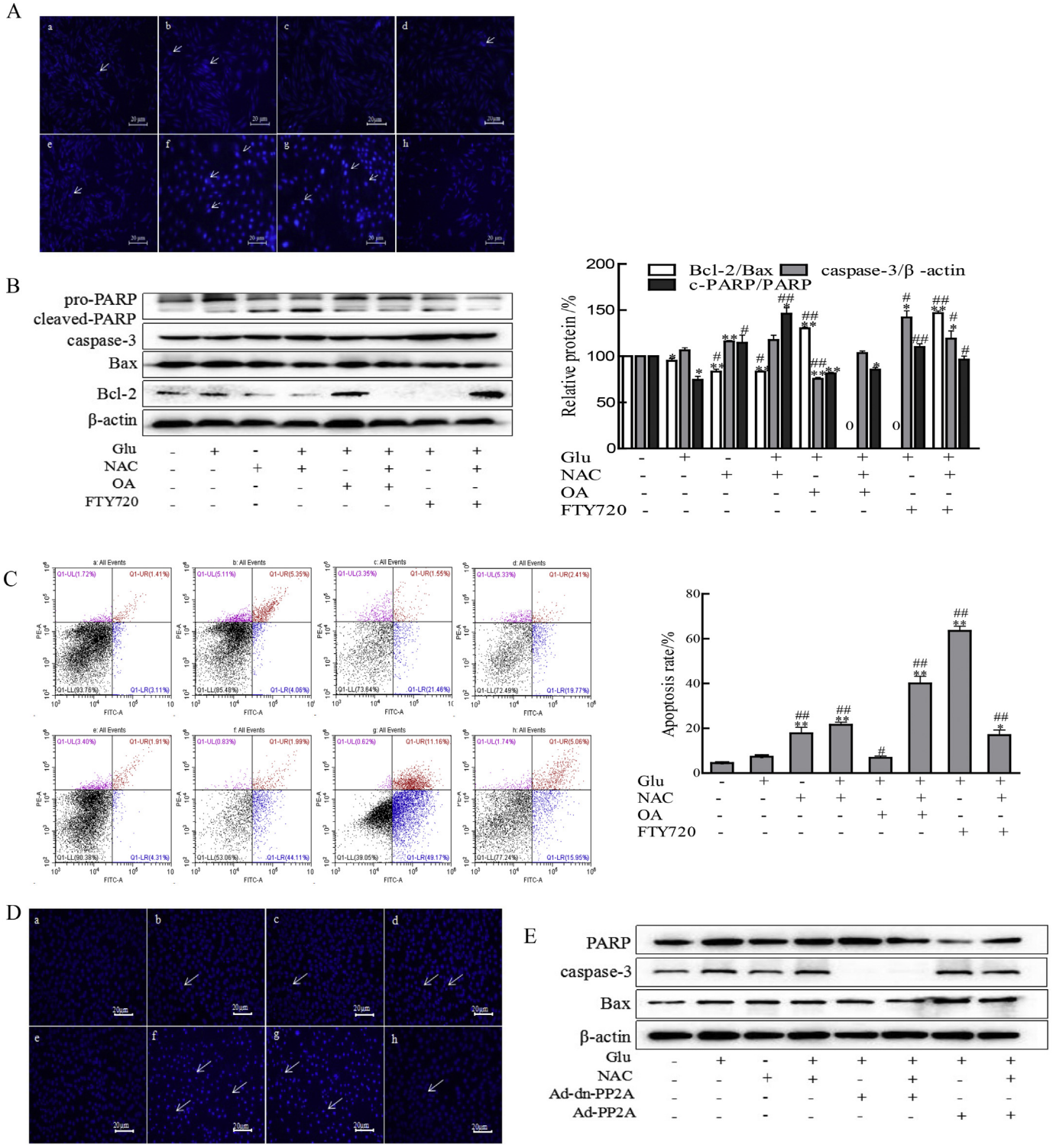

Fig. 5. Effects of PP2A/Nrf2 on high glucose induced apoptosis in H9c2 cells. H9c2 cells were pretreated without or with NAC (5 mmol/L) for 2 h, then treated with OA (20 nmol/L), FTY720 (5 mmol/L) or Ad-PP2A/Ad-dn-PP2A for 24 h, followed by treatment with glucose (50 mmol/L) for another 72 h. (A) Hoechst 33342 staining. Original magnification, × 200. Results are presented one of three independent experiments. (a) Control, (b) High glucose, (c) NAC, (d): NAC + high glucose, (e) OA + high glucose, (f) OA + NAC + high glucose, (g) FTY720 + high glucose, (h) FTY720 + NAC + high glucose. (B) Effects of PP2A and NAC on the expression of apoptosis related proteins in H9c2 cells. Western blotting was used to detect the expression of Bax, Bcl-2, caspase-3, and PARP. Results are presented as means ± SEM of three independent experiments. $^{*}P < .05$, $^{**}P < .01$, vs. Control; $^{\#}P < .05$, $^{\#\#}P < .01$, vs. high-glucose. (C) Apoptosis detection by flow cytometry. (a) Control, (b) High glucose, (c) NAC, (d) NAC + high glucose, (e) OA + high glucose, (f) OA + NAC + high glucose, (g) FTY720 + high glucose, (h) FTY720 + NAC + high glucose. Results are presented as means ± SEM of three independent experiments. $^{*}P < .05$, $^{**}P < .01$, vs. Control; $^{\#}P < .05$, $^{\#\#}P < .01$, vs. high-glucose. (D) Hoechst 33342 staining. Original magnification, × 200. Results are presented one of three independent experiments. (a) Control, (b) High glucose, (c) NAC, (d) NAC + high glucose, (e) Ad-dn-PP2A + high glucose, (f) Ad-dn-PP2A + NAC + high glucose, (g) Ad-PP2A + high glucose, (h) Ad-PP2A + NAC + high glucose. (E) Effects of Ad-PP2A and NAC on the expression of apoptosis related proteins in H9c2 cells. Western blotting was used to detect the expression of Bax, caspase-3 and PARP. Results are presented one of three independent experiments.

Table 1
The Changes of body weight and blood sugar levels in mice (means ± SD).

Project	Week	Control (n = 10)	Model (n = 11)	HG + OA (n = 10)	HG + FTY720 (n = 11)
Weight (g)	4	35.3 ± 4.1	36.8 ± 3.8	38.6 ± 3.8	39.0 ± 3.4
	5	38.6 ± 4.5	39.3 ± 3.5	41.0 ± 4.0	38.9 ± 3.5
	6	41.1 ± 2.7	42.3 ± 4.3*	44.6 ± 2.4**,#	40.9 ± 4.2*
Blood sugar (mmol/L)	4	5.9 ± 0.8	9.1 ± 0.8*	9.2 ± 0.98	9.3 ± 1.0*
	5	5.4 ± 1.0	10.9 ± 0.7*	11.0 ± 0.8	8.1 ± 1.3*
	6	5.3 ± 0.7	11.9 ± 0.8*	12.5 ± 0.7**,#	8.6 ± 1.1*,##

*P < .05, **P < .01, vs. Control group; #P < .05, ##P < .01, vs. Model group.

Table 2
The changes of oxidoreductases levels in serum (means ± SD).

Group	n	MDA(mmol/L)	SOD(U/ml)	MDA/SOD	CAT(U/g)	GSH-px(U)	NOS(U/ml)
Control	10	108.97 ± 12.52	15.39 ± 2.84	7.44 ± 1.74	33.85 ± 17.54	115.45 ± 19.43	1.22 ± 0.21
Model	11	136.42 ± 14.08	14.99 ± 1.55	9.36 ± 1.77*	16.62 ± 9.88*	120.08 ± 15.91	1.60 ± 0.52**
HG + OA	10	78.75 ± 7.97**,##	13.10 ± 3.94	6.86 ± 1.77*	32.65 ± 16.40#	116.23 ± 14.93	1.67 ± 0.14**
HG + FTY720	11	165.98 ± 16.38**,##	16.88 ± 2.38#	10.18 ± 2.99*	16.35 ± 7.95*	111.07 ± 14.59	1.50 ± 0.23*

*P < .05, **P < .01, vs. Control group; #P < .05, ##P < .01, vs. Model group.

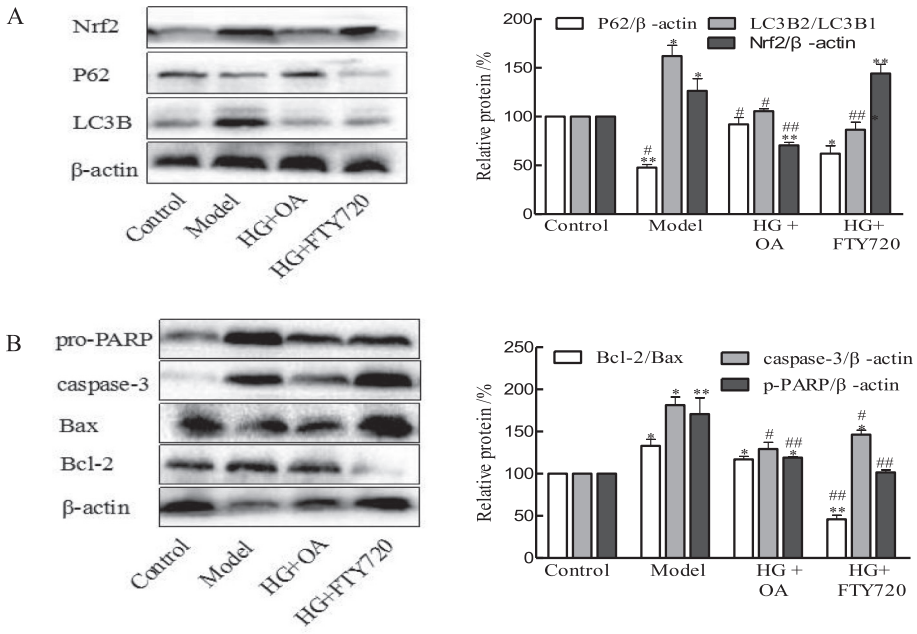

Fig. 6. Effects of PP2A on diabetes mellitus-related cardiomyopathy mice. (A and B) Western blotting was used to detect the expression of Nrf2, LC3B, P62 and apoptosis-related proteins such as Bax, Bcl-2, caspase-3, and PARP. Results are presented as means ± SEM of three independent experiments. *P < 0.05, **P < .01, vs. Control; #P < 0.05, ##P < .01, vs. Model.

autophagy under high glucose condition. While increasing PP2A expression and inhibiting ROS production, autophagy level decreased significantly. Commensurately, the expression of Nrf2 upregulated significantly when the expression of PP2A increased. This suggested that increasing the expression of PP2A in hyperglycemia can enhance cardiomyocyte protective autophagy, which is associated with antioxidant and reductive protein Nrf2. More recently, autophagy has been shown to engage in complex interplay with apoptosis. Apoptosis may begin with autophagy and autophagy can often end with apoptosis. Inhibition or a blockade of caspase activity may lead a cell to default into autophagic cell death from apoptosis [35]. It has been found that the binding of Bcl-2 to BH3 domain of Beclin 1 can inhibit autophagy [36]. Caspase can affect autophagy process by cleavage of autophagy related protein, especially p62 protein [37,38]. Ser70 phosphorylation of Bcl-2 by selective tyrosine nitration of PP2A-B56δ stabilizes its antiapoptotic activity [19]. Excess ROS could promote oxidative inactivation of protein phosphatase PP2A [18]. In our experiment, it was found that the expression of caspase-3 was increased under high glucose condition, and the apoptotic pathway was initiated, but the apoptosis of cardiomyocytes increased after inhibiting ROS by NAC. When the activity of PP2A was inhibited under high glucose condition, the expression of Bcl-2 and caspase-3 protein changed obviously, but the expression of Nrf2 decreased. After NAC was added to inhibit the production of ROS, the results showed a reverse trend.

The results of animal experiment were the same as that of cell experiments in vitro. Elevation of cardiomyocyte autophagy and inhibition of apoptosis was found in model group. By intraperitoneal injection of FTY720, it was found that myocardial injury of mice was improved. Compared with the model group, the expression of Nrf2 and autophagy increased significantly, while the expression of caspase-3 was increased and the expression of Bcl-2 was inhibited to promote cardiomyocyte apoptosis.

In conclusion, the role of PP2A/Nrf2 in DMCMP was studied for the first time and its mechanism was explored. It was found that the activity or expression of PP2A in DMCMP increased, and the myocardial protective autophagy increased, and apoptosis increased. Further studies had shown that this increased protective autophagy and apoptosis might be mediated by activating the antioxidant reduction pathway and

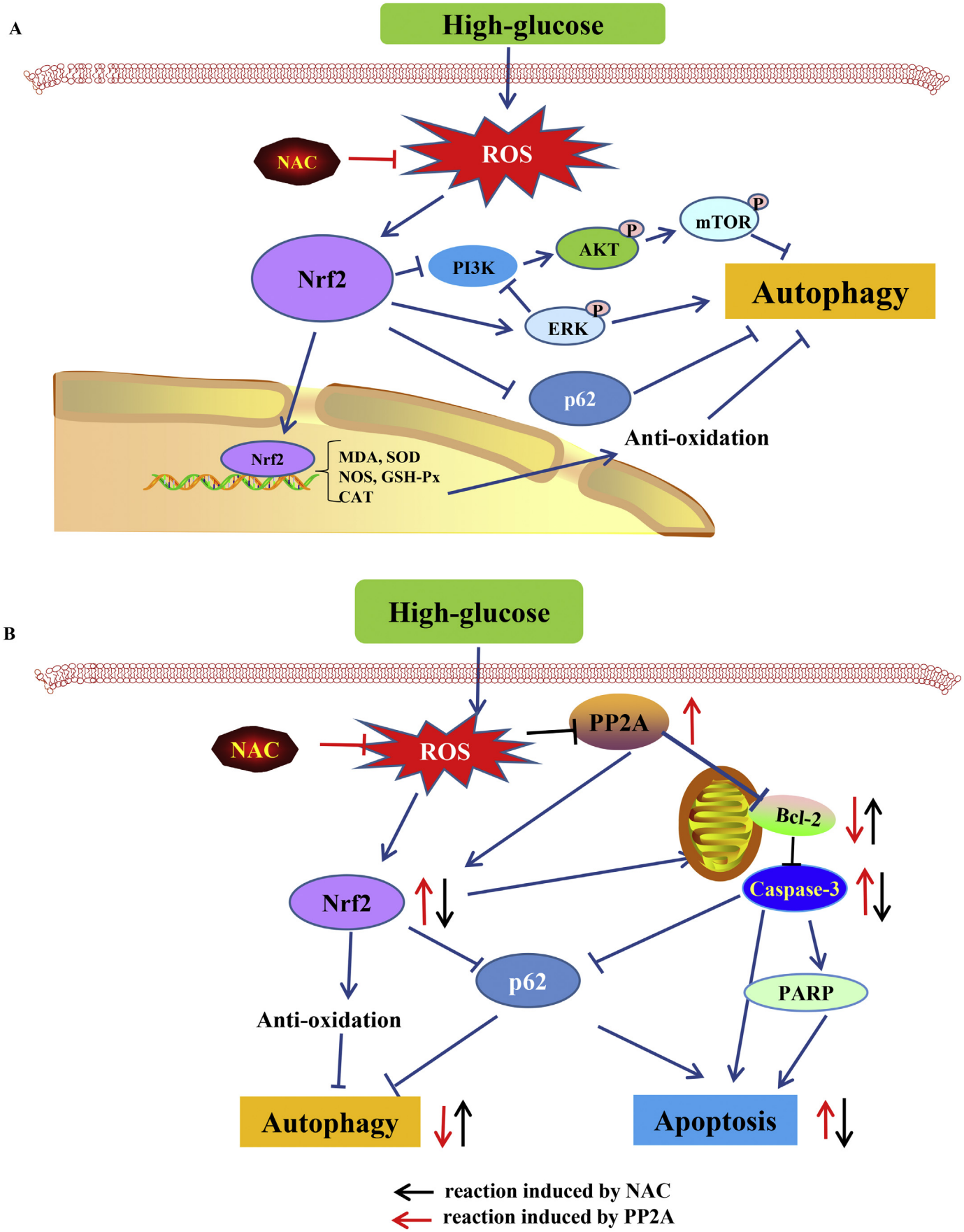

Fig. 7. Effects and mechanisms of PP2A/Nrf2 on high-glucose induced cardiomyopathy. (A) Regulation of high glucose on autophagy and apoptosis in high-glucose induced cardiomyopathy; (B) PP2A/Nrf2 regulates autophagy and apoptosis in high-glucose induced cardiomyopathy.

regulating the expression of Nrf2. The interrelation and regulation between PP2A and Nrf2 and the regulation of downstream autophagy and apoptosis by PP2A/Nrf2 may be related to ROS, p62, Bcl-2 and caspase-3 (Fig. 7B). This study will be helpful to explore the pathogenesis and mechanism of DMCMP and lay the foundation for the development of drugs for prevention and treatment of DMCMP.

Conflict of interests

The authors report no commercial or proprietary interest in any product or concept discussed in this article.

Acknowledgements

This work was supported by Key Research and Development Program of Shandong Province (No. 2016GSF201152) and Natural Science Foundation of Shandong Province (No. ZR2017MH028) of P. R. China. Ad-PP2A/Ad-dn-PP2A were presented by Professor Shile Huang, Health Sciences Center, Louisiana State University.

References

[1] P.M. Seferovic, W.J. Paulus, Clinical diabetic cardiomyopathy: a two-faced disease with restrictive and dilated phenotypes, Eur. Heart J. 36 (2015) 1718–1727.
[2] G. Jia, A. Whaley-Connell, J.R. Sowers, Diabetic cardiomyopathy: a hyperglycaemia- and insulin-resistance-induced heart disease, Diabetologia. 61 (2018) 21–28.
[3] M.M. Sung, S.M. Hamza, J.R. Dyck, Myocardial metabolism in diabetic cardiomyopathy: potential therapeutic targets, Antioxid. Redox Signal. 22 (2015) 1606–1630.
[4] G. Jia, M.A. Hill, J.R. Sowers, Diabetic cardiomyopathy: an update of mechanisms contributing to this clinical entity, Circ. Res. 122 (2018) 624–638.
[5] J. Chen, Z. Zhang, L. Cai, Diabetic cardiomyopathy and its prevention by nrf2: current status, Diabetes Metab. J. 38 (2014) 337–345.
[6] I. Falcão-Pires, A.F. Leite-Moreira, Diabetic cardiomyopathy: understanding the molecular and cellular basis to progress in diagnosis and treatment, Heart Fail. Rev. 17 (2012) 325–344.
[7] T. Suzuki, M. Yamamoto, Stress-sensing mechanisms and the physiological roles of the Keap1-Nrf2 system during cellular stress, J. Biol. Chem. 292 (2017) 16817–16824.
[8] A. Uruno, Y. Yagishita, M. Yamamoto, The Keap1-Nrf2 system and diabetes mellitus, Arch. Biochem. Biophys. 566 (2015) 76–84.
[9] S.K. Niture, R. Khatri, A.K. Jaiswal, Regulation of Nrf2-an update, Free Radic. Biol. Med. 66 (2014) 36–44.
[10] S. Murakami, H. Motohashi, Roles of Nrf2 in cell proliferation and differentiation, Free Radic. Biol. Med. 88 (2015) 168–178.
[11] J. Xu, S.R. Kulkarni, A.C. Donepudi, V.R. More, A.L. Slitt, Enhanced Nrf2 activity worsens insulin resistance, impairs lipid accumulation in adipose tissue, and increases hepatic steatosis in leptin-deficient mice, Diabetes. 61 (2012) 3208–3218.
[12] S. Kannan, V.R. Muthusamy, K.J. Whitehead, L. Wang, A.V. Gomes, S.E. Litwin, T.W. Kensler, E.D. Abel, J.R. Hoidal, N.S. Rajasekaran, Nrf2 deficiency prevents reductive stress-induced hypertrophic cardiomyopathy, Cardiovasc. Res. 100 (2013) 63–73.
[13] L. Li, J. Tan, Y. Miao, P. Lei, Q. Zhang, ROS and autophagy: interactions and molecular regulatory mechanisms, Cell. Mol. Neurobiol. 35 (2015) 615–621.
[14] Z.V. Varga, Z. Giricz, L. Liaudet, G. Haskó, P. Ferdinandy, P. Pacher, Interplay of oxidative, nitrosative/nitrative stress, inflammation, cell death and autophagy in diabetic cardiomyopathy, Biochim. Biophys. Acta 1852 (2015) 232–242.
[15] E.R. Lubbers, P.J. Mohler, Roles and regulation of protein phosphatase 2A (PP2A) in the heart, J. Mol. Cell. Cardiol. 101 (2016) 127–133.
[16] X.M. Ren, G.F. Zuo, W. Wu, J. Luo, P. Ye, S.L. Chen, Z.Y. Hu, Atorvastatin alleviates experimental diabetic cardiomyopathy by regulating the GSK-3β-PP2Ac-NF-κB signaling axis, PLoS One 11 (2016) e0166740.
[17] T. Shimura, M. Sasatani, K. Kamiya, H. Kawai, Y. Inaba, N. Kunugita, Mitochondrial reactive oxygen species perturb AKT/cyclin D1 cell cycle signaling via oxidative inactivation of PP2A in low dose irradiated human fibroblasts, Oncotarget. 7 (2016) 3559–3570.
[18] S. Nakahata, K. Morishita, PP2A inactivation by ROS accumulation, Blood. 124 (2014) 2163–2165.
[19] I.C. Low, T. Loh, Y. Huang, D.M. Virshup, S. Pervaiz, Ser70 phosphorylation of Bcl-2 by selective tyrosine nitration of PP2A-B56δ stabilizes its antiapoptotic activity, Blood. 124 (2014) 2223–2234.
[20] K.A. Coughlan, R.J. Valentine, N.B. Ruderman, A.K. Saha, Nutrient excess in AMPK downregulation and insulin resistance, J. Endocrinol. Diabetes Obes. 1 (2012) 1008.
[21] X.Z. Han, S. Gao, Y.N. Cheng, Y.Z. Sun, W. Liu, L.L. Tang, D.M. Ren, Protective effect of naringenin-7-O-glucoside against oxidative stress induced by doxorubicin in H9c2 cardiomyocytes, BioSci. Trends. 6 (2012) 19–25.
[22] I. Lakshmanan, S.K. Batra, Protocol for apoptosis assay by flow cytometry using Annexin V staining method, Bio. Protoc. 3 (2013) (pii: e374).
[23] Y. Teshima, N. Takahashi, S. Nishio, S. Saito, H. Kondo, A. Fukui, K. Aoki, K. Yufu, M. Nakagawa, T. Saikawa, Production of reactive oxygen species in the diabetic heart. Roles of mitochondria and NADPH oxidase, Circ. J. 78 (2014) 300–306.
[24] J. Gandhi, G. Dagur, K. Warren, N.L. Smith, S.A. Khan, Genitourinary complications of diabetes mellitus: an overview of pathogenesis, evaluation, and management, Curr. Diabetes Rev. 13 (2017) 498–518.
[25] M. Zhang, W.Z. Yu, X.T. Shen, Q. Xiang, J. Xu, J.J. Yang, P.P. Chen, Z.L. Fan, J. Xiao, Y.Z. Zhao, C.T. Lu, Advanced interfere treatment of diabetic cardiomyopathy rats by aFGF-loaded heparin-modified microbubbles and UTMD technique, Cardiovasc. Drugs Ther. 30 (2016) 247–261.
[26] G. Borghetti, D. von Lewinski, D.M. Eaton, H. Sourij, S.R. Houser, M. Wallner, Diabetic cardiomyopathy: current and future therapies. Beyond Glycemic control, Front. Physiol. 9 (2018) 1514.
[27] K. Huynh, B.C. Bernardo, J.R. McMullen, R.H. Ritchie, Diabetic cardiomyopathy: mechanisms and new treatment strategies targeting antioxidant signaling pathways, Pharmacol. Ther. 142 (2014) 375–415.
[28] K. Feidantsis, K. Mellidis, E. Galatou, Z. Sinakos, A. Lazou, Treatment with crocin improves cardiac dysfunction by normalizing autophagy and inhibiting apoptosis in STZ-induced diabetic cardiomyopathy, Nutr. Metab. Cardiovasc. Dis. 28 (2018) 952–961.
[29] S. Zhou, W. Sun, Z. Zhang, Y. Zheng, The role of Nrf2-mediated pathway in cardiac remodeling and heart failure, Oxidative Med. Cell. Longev. 2014 (2014) 260429.
[30] M. Li, A. Murabito, A. Ghigo, E. Hirsch, PI3Ks in diabetic cardiomyopathy, J. Cardiovasc. Pharmacol. 70 (2017) 422–429.
[31] P. Abeyrathna, Y. Su, The critical role of Akt in cardiovascular function, Vasc. Pharmacol. 74 (2015) 38–48.
[32] J. Gu, W. Hu, Z.P. Song, Y.G. Chen, D.D. Zhang, C.Q. Wang, Rapamycin inhibits cardiac hypertrophy by promoting autophagy via the MEK/ERK/Beclin-1 pathway, Front. Physiol. 7 (2016) 104.
[33] K.M. Mellor, M.E. Reichelt, L.M. Delbridge, Autophagic predisposition in the insulin resistant diabetic heart, Life Sci. 92 (2013) 616–620.
[34] Z. Xu, J. Sun, Q. Tong, Q. Lin, L. Qian, Y. Park, Y. Zheng, The role of ERK1/2 in the development of diabetic cardiomyopathy, Int. J. Mol. Sci. 17 (2016) E2001 pii.
[35] L.A. Booth, S. Tavallai, H.A. Hamed, N. Cruickshanks, P. Dent, The role of cell signalling in the crosstalk between autophagy and apoptosis, Cell. Signal. 26 (2014) 549–555.
[36] F. Zhou, Y. Yang, D. Xing, Bcl-2 and Bcl-xL play important roles in the crosstalk between autophagy and apoptosis, FEBS J. 278 (2011) 403–413.
[37] J.M. Norman, G.M. Cohen, E.T. Bampton, The in vitro cleavage of the hAtg proteins by cell death proteases, Autophagy. 6 (2010) 1042–1056.
[38] R. Ojha, M. Ishaq, S.K. Singh, Caspase-mediated crosstalk between autophagy and apoptosis: mutual adjustment or matter of dominance, J. Cancer Res. Ther. 11 (2015) 514–524.